







Design and Manufacturing of Microtextured Patient-Specific Coronary Stent

Francisco Franco-Martínez¹^a, William Solórzano-Requejo^{1,2}^b, Alejandro de Blas-de Miguel¹^c,
Matthias Vostatek³, Christian Grasl^{3,4}, Marta Bonora³^d, Francesco Moscato^{3,4,5}^e
and Andrés Díaz Lantada¹^f

¹*ETSI Industriales, Universidad Politécnica de Madrid, Madrid, Spain*

²*Department of Mechanical and Electrical Engineering, Universidad de Piura, Piura, Peru*

³*Center for Medical Physics and Biomedical Engineering, Medical University of Vienna, Vienna, Austria*

⁴*Ludwig Boltzmann Institute for Cardiovascular Research, Vienna, Austria*

⁵*Austrian Cluster for Tissue Regeneration, Vienna, Austria*


Keywords: Metasurfaces, Metamaterials, Additive Manufacturing, Coronary Artery Disease, Personalized Medicine.


Abstract: Currently, the most usual treatment for coronary artery disease is the use of stents, which are produced with standard dimensions and shapes and the surgeon selects the one that best fits the patient's anatomy. Due to this treatment, likelihood of restenosis might reach 40%. Additionally, thrombi formation is an important risk for these patients that is treated with anticoagulant medicines. Therefore, a design and manufacturing method to produce microtextured patient-specific coronary stent is developed with the aim to minimize the likelihood of restenosis and thrombosis. Stents consisting of unit cells structures that are regularly repeated to form a ring and, sometimes connectors to join the rings. To improve the fitting between artery and stent, parametric design of unit cell as a function of the length and mean radius of coronary artery is required. Then, the unit cell is microtextured to improve hemocompatibility using a bioinspired design in shark skin, which provide superhydrophobicity, drag reduction and oleophobicity under water conditions. Once the unit cell is micropatterned, a reverse engineering reconstruction is done to obtain the stent model. Finally, the design is manufactured with a 3D printer using two-photon polymerisation technology. SEM is used to evaluate the design and manufacturing method.


1 INTRODUCTION


Coronary artery disease is a major cause of mortality and morbidity (Ho et al., 2016), each year causes 3.9 million deaths in Europe and is estimated to cost the European Union €210 billion per year (*CVD Statistics*, n.d.). It occurs when fat, calcium and cellular debris accumulate in the artery wall blocking blood flow and causing an inadequate supply of oxygen and nutrients to the myocardium; resulting in infarction, cerebral hemorrhage, or ischemic stroke


(Pan et al., 2021). The most popular treatment is coronary angioplasty (CA), (Ho et al., 2016; Canfield & Totary-Jain, 2018). CA is a minimal invasive procedure used to expand the blood vessels and restore the function of the cardiovascular system by inserting a stent inside it. Constructively, coronary stents are small, complex, hollow and cylindrical-shaped tubes consisting of unit cells structures that are regularly repeated to form a ring; the ring, a group of unit cells that are held together; and the connectors, which join rings to build the stent.


^a  <https://orcid.org/0000-0002-7894-7478>

^b  <https://orcid.org/0000-0002-2989-9166>

^c  <https://orcid.org/0000-0003-2375-8327>

^d  <https://orcid.org/0000-0003-3667-0965>

^e  <https://orcid.org/0000-0003-0279-6615>

^f  <https://orcid.org/0000-0002-0358-9186>

The design of the components defines the biomechanical performance of the stent, the rings determine radial support and expandability; the number of connectors sets longitudinal stability, flexibility, and longitudinal integrity; and the reduced number of connectors provides greater flexibility and reduces arterial injuries (Polanec et al., 2020; Tomberli et al., 2018).

According to follow-up studies, 10% of patients require a replacement prosthesis one year after implantation and the likelihood of restenosis might reach 40% (Pan et al., 2021; Schillinger et al., 2007). These issues are the result from geometrical alterations in a coronary artery once surgery is done due to the size disparity between the blood vessel and the expanded stent which is manufactured with standard dimensions and shapes. A significant interaction force will be produced if the stent does not suit the diseased artery, injuring the artery and finally causing restenosis (Wang et al., 2018). This pathology is a major challenge and nowadays patients usually need anticoagulant and antiplatelet therapies (Movafaghi et al., 2019). Therefore, the combination of medical and mechanical design can improve notoriously the function of vascular prostheses and minimize the use of anticoagulant drugs to meet the needs of patients worldwide. Currently, many efforts are being made to minimize the risk of restenosis and thrombi formation, caused by the adsorption of plasma proteins and platelets adhesion, modifying the properties of the surface in contact with the blood applying controlled micro- and nanopatterns (Koh et al., 2010; Movafaghi et al., 2019).

Organisms as plants, animals and bacteria among others, has carried out different solutions to survive and adapt to the environment. The surface is where organisms interact with other organisms and the environment. Therefore, some of them has developed textured surfaces in micro and nanoscales with remarkable properties, such as the gecko, lotus flower or sharks. Regarding the need, it could be chosen one or another bioinspired microtexture and replicate it artificially.

Researchers have studied the use of superhydrophobic surfaces to improve the hemocompatibility. These surfaces are super-repellent to water with a static contact angle $> 150^\circ$ and minimum contact angle hysteresis $< 10^\circ$. Moreover, superhydrophobic surfaces present low blood protein adsorption and low blood cell interaction which leads to improve hemocompatibility (Movafaghi et al., 2019). Celik *et al.* demonstrated the use of biocompatible materials with superhydrophobic surfaces by manufacturing

samples rubbing the surface after coated the polydimethylsiloxane (PDMS) with carnauba wax. The static (169°) and sliding (3° and 5° respectively) contact angle measurements with water and blood showed super-repellency. Additionally, they studied the contact angle with platelets suspension, erythrocyte concentrate and fresh plasma, all of them showed superhydrophobic behaviour (Celik et al., 2021).

Hoshian *et al.*, also used PDMS with microtextured inner surface coated with titania (TiO_2) to produce flexible tubes which repel water and blood, where the blood contact angle for the microtextured surface was $161 \pm 3^\circ$ compared with the control surface (flat PDMS/titania surface) of $90 \pm 2^\circ$. The improvement in repellency is notorious. Furthermore, they investigated the drag reduction when tubes were microtextured compared with no-textured tubes obtaining only 39% and 99% respectively, when both measurements were compared to a free falling droplet in air. Finally, some test were performed comparing the superhydrophobic surface with smooth titania and PDMS substrate revealing that only the superhydrophobic one does not present adhered platelets (Hoshian et al., 2017).

Considering the main causes of restenosis and thrombi formation, in this study the potential of designing and manufacturing a patient-specific microtextured stent based on the disease will be demonstrated by designing two patient-specific stents, micropatterning and manufacturing one of them to test the feasibility of the design methodology presented above. The shark skin micropattern is selected because his drag reduction under water condition, superhydrophobicity in air with contact angle 155° and oleophobicity in water environment (Jung & Bhushan, 2009). It will be show a novelty method to microtextured stents with the aim of reducing restenosis and thrombi formation.

2 MATERIALS AND METHODS

2.1 Open-Source Coronary Stent Design

Parametric design is one of the methods to produce stents for each patient since it can effectively improve their mechanical properties. For this purpose, the parameterization of two coronary stents as a function of the length (L) and mean radius (R) of the artery is detailed. The first design is distinguished because the unit cells are joined together, whereas in the second they are linked by connectors.

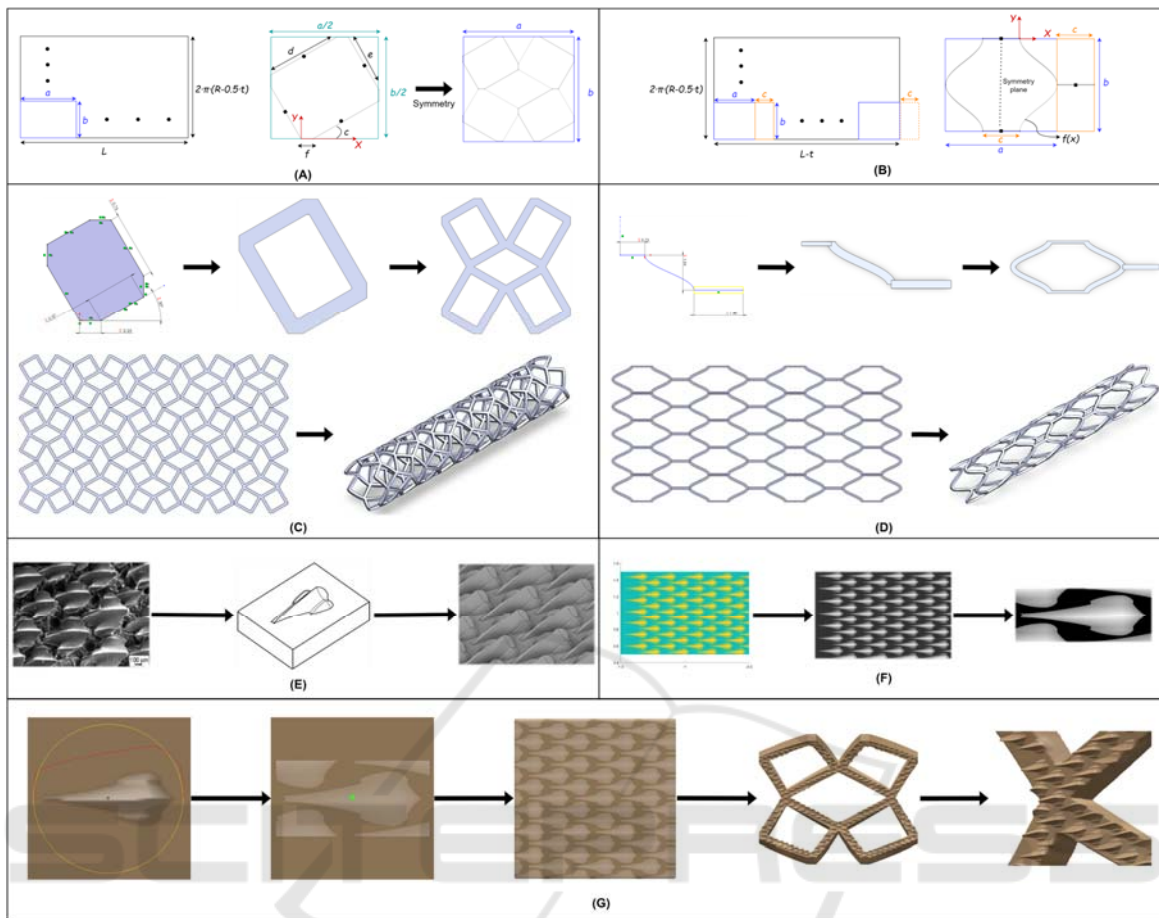


Figure 1: Macro and microstructure design. CAD design process of the (A, C) first and (B, D) second coronary stents. (E) Bioinspired microstructures CAD design. (F) Mask acquisition. (G) Surface texturing.

2.1.1 First Design Strategy

The parameterization of the first model starts with the development of a hollow cylinder; a rectangle of width equal to L and length, to the average length of the artery minus the half of the stent thickness ($2\pi \cdot (R - 0.5t)$). Macroscopically, the unit cell is another rectangle of “ a ” width and “ b ” length embedded in the development to be repeated “ N_x ” and “ N_y ” times in the longitudinal (X) and radial (Y) axes respectively (Figure 1A). With these similarities, the first equivalences are made:

$$a = \frac{L}{N_x} \quad (1)$$

$$b = \frac{2 \cdot \pi \cdot (R - 0.5 \cdot t)}{N_y} \quad (2)$$

From the microscopic point of view, the unit cell has a defined shape delimited by the rectangle “ ab ” (Figure 1A). Hence, the geometric relationships

between the macro and microscopic parameters must be expressed mathematically, considering that there is a more basic unit that with even and odd symmetry constitutes the unit cell of the stent:

$$\frac{a}{2} = d \cdot \cos(c) + e \cdot \sin(c) + f \quad (3)$$

$$\frac{b}{2} = d \cdot \sin(c) + e \cdot \cos(c) + f \quad (4)$$

The parameters “ a ” and “ b ” are constrained by the artery dimensions (L and R) and the designer controls “ N_x ”, “ N_y ” and “ t ” to obtain the best performance. So, the other variables are unknowns, but there are only two equations ((3) and (4)) resulting in an indeterminate system; therefore, it is considered that the unit cell opening, quantified through the angle “ c ”, is a parameter regulated by the designer and “ f ” is equal to “ t ” to make its cross-section a square. By partially solving the system of equations:

$$m1 = d + e = \frac{a + b - 4 \cdot f}{2 \cdot (\sin(c) + \cos(c))} \quad (5)$$

$$m2 = e - d = \frac{a - b}{2 \cdot (\sin(c) - \cos(c))} \quad (6)$$

The microscopic variables “ d ” and “ e ” are a combination of “ $m1$ ” and “ $m2$ ”

$$d = \frac{m1 - m2}{2} \quad (7)$$

$$e = \frac{m1 + m2}{2} \quad (8)$$

All these parameters are imported in the “Equations” command, as global variables, in SolidWorks 2021[®] (Dassault Systèmes, Waltham, MA, USA). This software is used for its simplicity when modelling complex geometries because the parameterization of parts is highly optimized, and its interface is user-friendly.

For the modelling, a sketch is made in the “Right plane” correctly defining the constraints to obtain the geometrical changes under the modification of the global variables. Then, it is extruded with a depth equal to “ t ” and the “Shell” tool allows get an internal wall with same thickness. To compose the unit cell from this basic structure, the “Symmetry” tool is used and the “Linear Pattern” command replicates “ Nx ” and “ Ny ” times the unit cell in the X and Y axes to elaborate a mesh, development of the coronary stent. Finally, the “Flex” and “Combine” tool folds the mesh and joins each unit cell to form the coronary stent (Figure 1C).

2.1.2 Second Design Strategy

The design of the second model starts from the same development but, in addition to the unit cell, the connectors that link them must be parameterized. Therefore, both elements are integrated forming a larger unit cell that is repeated bidirectionally. From Figure 1B, the large-scale equivalence is performed:

$$L - t = Nx \cdot (a + c) - c \quad (9)$$

$$b = \frac{2 \cdot \pi \cdot (R - 0.5 \cdot t)}{Ny} \quad (10)$$

This system has three unknowns (“ a ”, “ b ” and “ c ”) and only two equations. Therefore, it is indeterminate and one of the unknown variables must be defined. Due to the symmetry of the design, the width of the unit cell was related to the length of the connector:

$$c = \frac{a}{3} \quad (11)$$

As a result, introducing equation (11) in (9) we obtain:

$$a = \frac{L - t}{4/3 \cdot Nx - 1/3} \quad (12)$$

Unlike the previous case, the thickness also affects the longitudinal axis with the term $(L - t)$ appearing in equation (12), a consequence of the unit cell geometry, which is modelled in SolidWorks[®] through sine function:

$$f(x) = \frac{c}{2} \cdot \sin\left(\frac{2\pi}{b} \cdot \left(x - \frac{b}{4}\right)\right) + \frac{c}{2}; x \in [0, 0.5b] \quad (13)$$

The above equations are imported into the Solidworks[®] file as global variables. The sinusoidal structure and its connector are sketched at the origin of the “Top plane” and the “Swept Boss/Base” command is used to obtain them three-dimensionally with square cross-section of side “ t ”. Furthermore, a double symmetry is performed to produce the complete unit cell. Then, the “Linear Pattern” tool replicates the cell “ Nx ” and “ Ny ” times, but the connector only “ $Nx - 1$ ” times because the stent must start and end with the unit cell. Once the mesh is prepared, the elements are folded and combined to form the vascular prosthesis (Figure 1D).

2.2 3D Coronary Artery Model

A STL file of an artery (Model ID 3DPX-012589), based on a CT scan and segmented by researchers at the University of Toronto and Toronto General Hospital, has been downloaded from the NIH 3D Print Exchange repository (*Phantom Coronary Artery Models / NIH 3D Print Exchange*, n.d.) to quantify its length and average radius, being 22 and 1.71 mm respectively. Accordingly, the two coronary stent models described above are adapted to extract the unit cell and connector in the final position for texturing.

2.3 Attainment of Microtextures

To create a microtexture to pattern the inner surface of the stent, three different steps are required, from the bioinspired microtexture to patterning the surface with it (Figure 1E-G). The design process followed to create the microtextured stent is described in detail in (Franco-Martínez et al., 2022) where the authors explained a design methodology to pattern the 3D objects surfaces.

2.3.1 Microtexture Selection and Computer Aided Design (CAD)

Previous studies showed that superhydrophobic surfaces enhance hemocompatibility. Consequently, shark skin is an adequate surface with the required attribute. In this study, bioinspired shark skin replica from (Jung & Bhushan, 2009) was chosen (first image shown in Figure 1E) because of its high similarity to nature, complex shape, high superhydrophobicity and the authors provided the dimensions of replicated shark scales. Then, one image and dimensions are required to replicate the shape in CAD software, obtaining a bioinspired surface model. Autodesk Inventor 2021[®] (Autodesk, Inc.) was used to design the pattern; to replicate the chosen shape, one bioinspired shark scale is done using the “loft” tool twice. Afterwards, this single model is replicated along a flat surface with the “Pattern sketch driven” command (Figure 1E).

2.3.2 Mask Acquisition

A grayscale mask is required to transfer the designed pattern to the unit cell that works as the base for the stent. Matlab R2022a[®] (Mathworks, Inc.) was used to convert the STL file with shark skin pattern into a grayscale mask. The STL is imported by “stlread” tool, plotted with “patch” tool, transformed into an image in grayscale with “rgbtogray” command and “rescale” function is used to obtain the final mask with better resolution. Finally, the image is trimmed and saved to use in the next step (Figure 1F).

2.3.3 Surface Texturing

Once the unit cell is designed in CAD, the STL file is imported to 3D Coat V4.9.65[®] (Pilgway). This software offers a wide range of tools for digital sculpting over the STL by “displacement mapping”, a method that apply height maps to displace the points or voxels of the mesh.

Regarding that, the shark skin mask is imported as image in 3D Coat. Displacement’s height is directly proportional to intensity in gray scale. The mask is projected from the front view and it is used as template over the surface micropatterned with the chosen brush, determined by shape (in this case shark scale), height and radius. To sculpt the surface, “live clay” tool is used, which allows to add more density of triangles where it is required on the surface to achieve micrometer and well-defined range of the micropatterning.

2.3.4 Manufacturing Process

Technology used to manufacture the stent prototype is two-photon polymerisation (2PP), NanoOne (UpNano GmbH, Vienna, Austria). It is a lithography process capable of generating 3D structures with nanometer feature sizes. The model was prepared in Think3D (UpNano GmbH, Vienna, Austria) and printed with UpPhoto (2-photon resin, UpNano) which is biocompatible and non-cytotoxic (Materials – UpNano – High-Resolution 3D Printing, n.d.), in printing mode “vat” with a laser power of 250 mW at a writing speed of 750 mm/s. To save time infill mode “coarse” is selected and structuring was done in one step with Fluar 5x/0.25 objective (Carl Zeiss Microscopy, New York, United States).

After printing, the sample was rinsed in isopropyl alcohol and air dried. A scanning electron microscopy (SEM) (Zeiss EVO MA10, Oberkochen, Germany) was used for imaging, and previously, the sample was gold coated with a Quorum Q150R ES sputter coater (Quorum Technologies Ltd, Laughton, United Kingdom). Manufacturing and imaging process followed in this study is similar to (Franco-Martínez et al., 2022).

3 RESULTS

3.1 Micropatterning Unit Cell

Figure 2, shows the micropatterned unit cell demonstrating the possibility of patterning 3D object with curved surfaces. Due to the performance of 3D Coat, the dimensions of the textures in CAD (Figure 2A) and 3D Coat (Figure 2B) varied a few microns because of the size and place of the mesh triangles, as it is commented in section 2.3.3. It is assumed that this deviation will not affect the superhydrophobicity state, since the fabrication creates the same or more due to its accuracy. Additionally, the imprecisions could enhance hemocompatibility thanks to produce a non-uniform area, as shown in (Koh et al., 2010) when the high aspect ratio textures are deformed and bent complicating the adhesion of platelets.

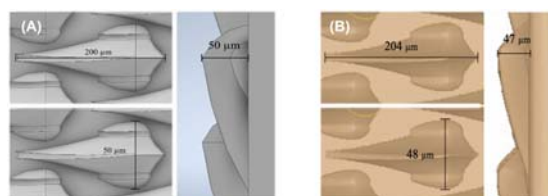


Figure 2: (A) CAD microtextures with dimensions. (B) 3D Coat microtextures with dimensions.

3.2 Reverse-Engineered Reconstruction of Microtextured Stent

From the textured unit cell, the coronary stent is reconstructed. First, the cell is replicated “ N_y ” times radially to form the ring, which is then cloned “ N_x ” times linearly to assemble the patient-specific textured coronary stent, whose length and outer radius are equal to the artery dimensions (Figure 3). However, in the second model, the connector is replicated only “ $N_x - 1$ ” times due to its design (section 2.1).

This simplicity in the reconstruction is a consequence of the macroscopic and microscopic view explored in the computational design of coronary stents.

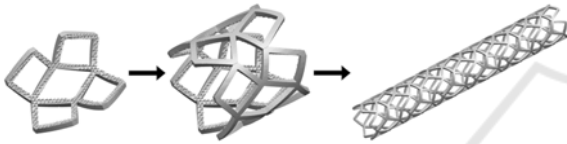


Figure 3: Reconstruction of textured coronary stents.

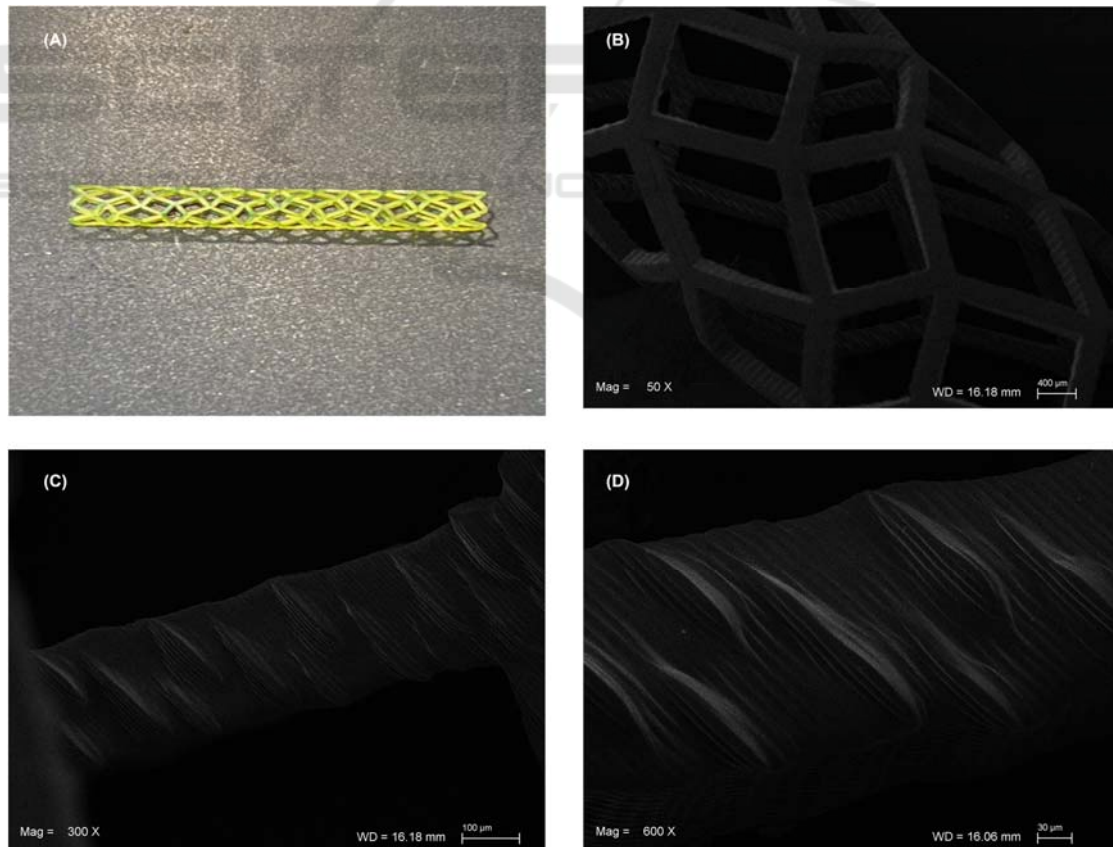


Figure 4: Microtextured Stent. (A) Real prototype. (B) SEM image outer surface with 50x magnification. SEM images inner microtextured surface (C) 300x and (D) 600x magnification.

3.3 Microtextured Stent Manufacturing

3D manufacturing process is used to fabricate the microtextured first design strategy stent prototype (Figure). The second design (Figure 1B) has not been manufactured yet.

The microtextured stent prototype can be observed in Figure . It is shown the inner surface microtextured with remarkable shark’s scales, despite of the sides riblets cannot be seen in most of them (Figure D). Indeed, the stent was printed in “vat” mode with infill “coarse” which is very fast and the printing time was 20 minutes approximately. It is feasible to reach higher accuracy with more precise objective and longer printing time.

This prototype demonstrates that 3D objects with complex and controlled surface topography can be manufactured. In literature, most of microstructures are made on a flat surface, as done in (Koh et al., 2010), (Celik et al., 2021) or (Jung & Bhushan, 2009).

Hoshian *et al.* developed a manufacturing process to design flexible tubes with microstructures on inner surface. However, the structures were completely random in shapes and position, in contrast to the 2PP

printing process that allows controlled and complex structures to be made.

Regarding the material employed, despite its biocompatibility, it may not be appropriate to use as a stent due to its mechanical properties. In this case, authors believe that it is feasible to use it as a template, manufacturing the final stent in another material, for example by applying the process developed in (Hoshian et al., 2017). The material, interaction with blood and implantation have to be investigated in following studies.

4 CONCLUSIONS

In this study, a patient-specific microtextured stent was designed and manufactured to minimize restenosis and thrombi formation without the use of anticoagulant medicines, whose design process is characterized by its low computational and time cost, due to the exposed three-dimensional object modelling and texturing strategies.

Based on the design strategies described above, considering their macroscopic (development) and microscopic (unit cell and connector) view, it is possible to computationally model any type of coronary stent. Furthermore, the parameterization favors the customization of these biodevices, since the equation approach is a function of the length and mean radius of the artery. Shark scales is well-known because its drag reduction and superhydrophobicity in air conditions. Additionally, it is oleophobic under water conditions. Therefore, the authors chose it as bioinspired microtexture for the inner surface and believe that this topography is interesting because its oleophobic behaviour. If the microstructures reach oleophobicity under blood conditions, the adsorption of proteins will not be possible and, consequently, platelets adhesion will be reduced.

Finally, the authors demonstrated that it is possible to design complex micropatterns on 3D objects through this study of the stent. Even this novel method could be applied to texture other implants with different patterns, such as tracheal stents, grafts or dental implants to achieve better biocompatibility and avoid problems after surgery. However, it should be noted that the study in its current form is mainly the design process. Indeed, according to the European Medical Devices Regulation 2017/745, customized implants cannot reach patients without prescription and involvement in the design procedure of physicians and surgeons, therefore, this research brings an engineering point of view. Consequently, before the presented designs can be considered

successful solutions, collaboration with healthcare personnel would be essential to improve the work by taking into account the problems that may arise in the pre-, intra- and postoperative phases; and by performing systematic in vitro and in vivo evaluations.

ACKNOWLEDGEMENTS

This research study has been funded by the European Union's Horizon 2020 Research and Innovation Programme under grant agreement No. 953134 (INKplant project: *Ink-based hybrid multi-material fabrication of next generation implants*).

"Optimized Hydrodynamic Flow Behaviour by Selective Surface Structured of Ceramic 3D Printed Rotodynamic Blood Pumps - OPTIFLOW-3D" funded by the Austrian Research Promotion Agency (FFG), Nr. 891239.

REFERENCES

- Canfield, J., & Totary-Jain, H. (2018). 40 Years of Percutaneous Coronary Intervention: History and Future Directions. *Journal of Personalized Medicine*, 8(4), Article 4. <https://doi.org/10.3390/jpm8040033>
- Celik, N., Sahin, F., Ruzi, M., Yay, M., Unal, E., & Onses, M. S. (2021). Blood repellent superhydrophobic surfaces constructed from nanoparticle-free and biocompatible materials. *Colloids and Surfaces B: Biointerfaces*, 205, 111864. <https://doi.org/10.1016/j.colsurfb.2021.111864>
- CVD Statistics*. (n.d.). Retrieved 29 December 2022, from <https://ehnheart.org/cvd-statistics.html>
- Franco-Martinez, F., Grasl, C., Kornfellner, E., Vostatek, M., Cendrero, A. M., Moscato, F., & Lantada, A. D. (2022). Hybrid design and prototyping of metamaterials and metasurfaces. *Virtual and Physical Prototyping*, 17(4), 1031–1046. <https://doi.org/10.1080/17452759.2022.2101009>
- Ho, M.-Y., Chen, C.-C., Wang, C.-Y., Chang, S.-H., Hsieh, M.-J., Lee, C.-H., Wu, V. C.-C., & Hsieh, I.-C. (2016). The Development of Coronary Artery Stents: From Bare-Metal to Bio-Resorbable Types. *Metals*, 6(7), Article 7. <https://doi.org/10.3390/met6070168>
- Hoshian, S., Kankuri, E., Ras, R. H. A., Franssila, S., & Jokinen, V. (2017). Water and Blood Repellent Flexible Tubes. *Scientific Reports*, 7(1), 16019. <https://doi.org/10.1038/s41598-017-16369-3>
- Jung, Y. C., & Bhushan, B. (2009). Wetting Behavior of Water and Oil Droplets in Three-Phase Interfaces for Hydrophobicity/philicity and Oleophobicity/philicity. *Langmuir*, 25(24), 14165–14173. <https://doi.org/10.1021/la901906h>

- Koh, L. B., Rodriguez, I., & Venkatraman, S. S. (2010). The effect of topography of polymer surfaces on platelet adhesion. *Biomaterials*, *31*(7), 1533–1545. <https://doi.org/10.1016/j.biomaterials.2009.11.022>
- Materials – UpNano – high-resolution 3D printing. (n.d.). Retrieved 31 October 2022, from <https://www.upnano.at/materials/>
- Movafaghi, S., Wang, W., Bark, D. L., Dasi, L. P., Popat, K. C., & Kota, A. K. (2019). Hemocompatibility of super-repellent surfaces: Current and future. *Materials Horizons*, *6*(8), 1596–1610. <https://doi.org/10.1039/C9MH00051H>
- Pan, C., Han, Y., & Lu, J. (2021). Structural Design of Vascular Stents: A Review. *Micromachines*, *12*(7), 770. <https://doi.org/10.3390/mi12070770>
- Phantom Coronary Artery Models | NIH 3D Print Exchange. (n.d.). Retrieved 11 April 2022, from <https://3dprint.nih.gov/discover/3dpx-012589>
- Polanec, B., Kramberger, J., & Glodez, S. (2020). A review of production technologies and materials for manufacturing of cardiovascular stents. *Advances in Production Engineering & Management*, *15*(4), 390–402. <https://doi.org/10.14743/apem2020.4.373>
- Schillinger, M., Sabeti, S., Dick, P., Amighi, J., Mlekusch, W., Schlager, O., Loewe, C., Cejna, M., Lammer, J., & Minar, E. (2007). Sustained Benefit at 2 Years of Primary Femoropopliteal Stenting Compared With Balloon Angioplasty With Optional Stenting. *Circulation*, *115*(21), 2745–2749. <https://doi.org/10.1161/CIRCULATIONAHA.107.688341>
- Tomberli, B., Mattesini, A., Baldereschi, G. I., & Di Mario, C. (2018). Breve historia de los stents coronarios. *Revista Española de Cardiología*, *71*(5), 312–319. <https://doi.org/10.1016/j.recesp.2017.11.016>
- Wang, Q., Fang, G., Zhao, Y.-H., & Zhou, J. (2018). Improvement of Mechanical Performance of Bioresorbable Magnesium Alloy Coronary Artery Stents through Stent Pattern Redesign. *Applied Sciences*, *8*(12), 2461. <https://doi.org/10.3390/app8122461>